

## Structural and Fractographic Analysis of Aluminum Alloy before and after Fatigue Loading

Milan Uhrčík (0000-0002-2782-5876), Peter Palček (0000-0001-7902-2007), Mária Chalupová (0000-0003-0175-9484), Lenka Kuchariková (0000-0002-2688-1075), Lucia Pastierovičová (0000-0001-5341-9292), Denisa Medvecká (0000-0002-0553-885X), Lenka Markovičová (0000-0002-1129-5532), Róbert Balšianka, Alan Vaško (0000-0002-3937-2691)

Department of Materials Engineering, Faculty of Mechanical Engineering, University of Žilina. Univerzitná 8215/1, 01026 Žilina. Slovakia. E-mail: milan.uhrick@fstroj.uniza.sk, peter.palcek@fstroj.uniza.sk, maria.chalupova@fstroj.uniza.sk, lenka.kucharikova@fstroj.uniza.sk, lucia.pastierovicova@fstroj.uniza.sk, denisa.medveckea@fstroj.uniza.sk, lenka.markovicova@fstroj.uniza.sk, alan.vasko@fstroj.uniza.sk

The article is focused on the analysis of the structure and fracture surface of aluminum alloy specimens. Aluminum alloy AlMg9 was mainly used as an experimental material. The material from which specimens were made was supplied as cast without heat treatment, and specifically the material was produced by the continuous casting method. The structure of the test material was examined using a Neophot 32 optical microscope, and the fracture surface of the test specimen was examined using a scanning electron microscope (SEM). The fatigue life of the aluminum alloy was tested by method of a three-point bending cyclic loading using the parameters - frequency  $f = 100$  Hz, temperature  $T = 22 \pm 5$  °C and stress ratio  $R = 0.11$ . The analysis showed that cast aluminum alloys are very sensitive to casting defects, such as porosity or the content and distribution of intermetallic phases. If large pores or phases are present on or near the surface of the sample, this can be the dominant cause of fatigue crack initiation and reduction of the fatigue lifetime.

**Keywords:** Aluminum Alloy, Fracture Surface, Structure, Fatigue, Bending Loading

### 1 Introduction

The automotive industry currently uses a wide range of aluminum alloys to produce components used in powertrains and chassis including transmission housings, inlet manifolds, cylinder heads, wheels, engines, but also as decorative elements. The increasing trend of replacing steel parts with lighter aluminium ones has caused aluminum alloys to be widely used in other areas of the automotive industry [1, 2].

Aluminum–magnesium casting alloys are mainly used for production of automotive safety parts due to their low density, resulting in the reduction of castings, but magnesium's strong oxidation and poor formability have limited its use. For this reason, it is urgent to develop casting alloys with higher strength and perspective to produce automotive parts with high shape integrity that can be subjected to cyclic stress, such as subframe and door frame. Excellent mechanical properties of Al–Mg alloys, for example with the addition of Si, and low production costs determined this alloy to be chosen as a structural material in the production of most industrial products, especially for the production of structural components in the automotive industry [1, 3].

Aluminum alloy castings have been increasingly

used in recent decades, along with the industry's tendency to create new ways to downsize and improve properties. The quality factor is based on the development and application of new compounds and alloys, as well as on many methods of investigating their properties and uses [4].

Properties of the cast products, such as quality, are mainly affected by microstructural changes during the crystallization process of the melted alloy. It is very important and beneficial to understand the phase formation during the casting process to obtain desired material properties [1].

The fatigue process can be generally divided into two main steps [5]. The first step is the initiation of microcracks due to local accumulation of dislocations, high stress at local points, plastic deformation around inhomogeneous inclusions or other imperfections. And the second step is the propagation of cracks that cause permanent damage. The position and mode of fatigue crack initiation depends on the geometry of the sample, the microstructure of the material and of course also on the type of applied stress [5, 6]. Crack initiation periods can be very different and cracks can form either at the surface or below the surface. The initiation of fatigue cracks can be observed at stress concentration points where there is an area of least resistance. The number of cycles required for

fracture ( $N_f$ ) can be determined from the number of stress cycles required for the initial crack to appear in the material ( $N_i$ ) and the number of stress cycles, required for a crack to propagate from the initial length to the critical length ( $N_p$ ) when the final failure can be expected to occur ( $N_f = N_i + N_p$ ) [5].

Aluminum alloy castings usually contain various structural discontinuities that have a significant impact on the strength and fatigue life of these alloys [7].

The manuscript presents study and analysis of aluminum alloy for the casting type of Al-Mg, especially an aluminum alloy AlMg9. Experimental

measurement is aimed at structural evaluation and fractographic analysis of fracture surfaces after fatigue loading.

## 2 Experimental material

A commercial aluminum cast alloy of the Al-Mg type (AlMg9) was used as an experimental material, which was supplied by its respective manufacturer in the form of an ingot (Fig. 1), in a cast state and without heat treatment. The ingot was produced by the method of continuous casting. From this ingot, simple block specimens with dimensions of 18 mm x 10 mm x 40 mm (w x h x d) were cut and milled.

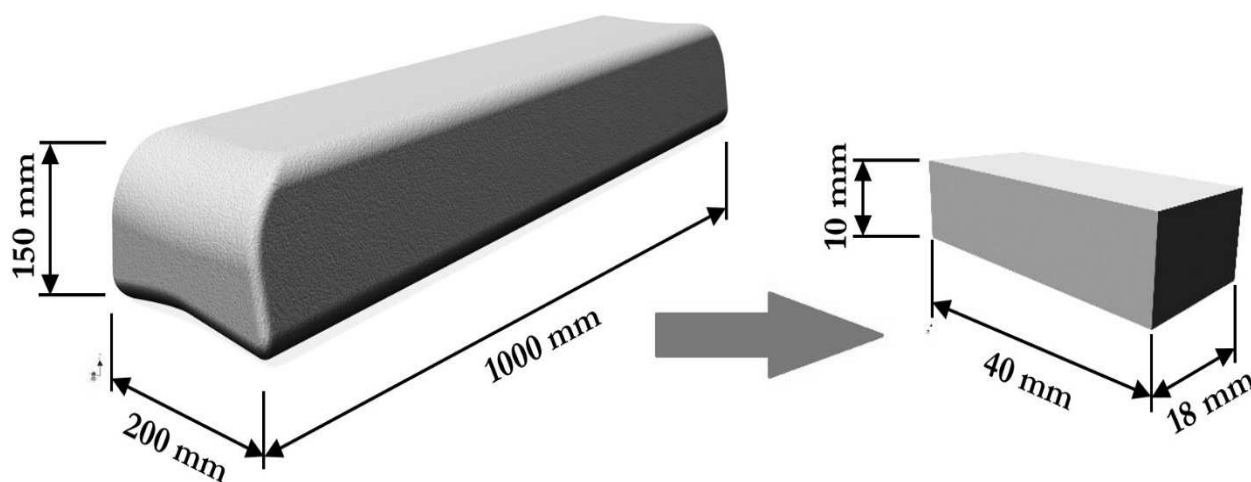


**Fig. 1** An ingot of aluminum cast alloy and a specimen

### 2.1 Material

After the delivery of the ingot, a spectral analysis was performed by a SPECTROMAXx spark emission

spectrometer to determine the exact chemical composition of the aluminum cast alloy. The determined chemical composition is shown in the Table 1.

**Tab. 1** Determined chemical composition of the aluminium cast alloy (in wt.%)

	Cu	Cr	Fe	Mg	Mn	Ni	Pb	Si	Al
<b>AlMg9</b>	0.003	0.006	0.103	9.457	0.403	0.004	0.029	1.306	balance

This material is known for its excellent corrosion resistance, it can be machined, polished and welded very well. The advantage of this alloy is that it can be used without any heat treatment, which can save the costs of manufacturing various parts and whole components from this material. The production of this alloy is mainly mediated by the high-pressure casting method [8].

### 2.2 Microstructure

Before the fatigue tests, the experimental material was first subjected to metallographic analysis. The microstructure was studied using a Neophot 32 optical

microscope and a TESCAN Vega II LMU scanning electron microscope with a Brucker-Quantax analyzer. The microstructure was in the initial state and was prepared by deep etching [9 - 11].

The microstructure of the aluminum cast alloy was significantly dendritic (Fig. 2). The structure was formed mainly by the matrix of phase  $\alpha$ , what is a solid solution of additive elements in aluminum. The microstructure also contained  $Mg_2Si$  intermetallic phases,  $\beta$  phases ( $Al_3Mg_2$ ) and other phases formed by a combination of additive elements in aluminum, for example, an iron phase ( $Al_6(FeMn)$ ). All phases were located mainly in the interdendritic areas.

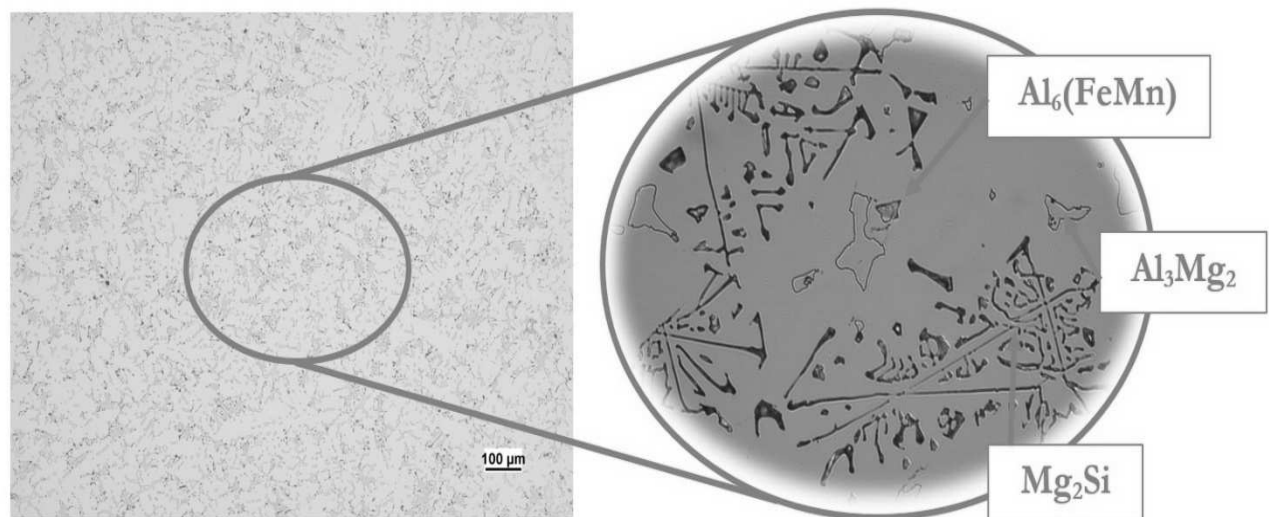


**Fig. 2** The microstructure of the investigated aluminum cast alloy AlMg9

As part of the microstructural analysis, a quantitative evaluation of the structure was also performed, which included a percentage evaluation of shares of individual phases present in the microstructure. This evaluation was performed on a Neophot 32 optical microscope using a NIKON Coolpix 4500 camera and NIS Elements software. Percentage evaluation of shares of individual phases (Fig. 3) was carried out at

1000x magnification and the specimen was etched with 0.5% hydrofluoric acid. The largest share of the structure was the  $\beta$  phase (8.6%), then it was the  $\text{Mg}_2\text{Si}$  intermetallic phase with a share of 7.1% and finally the  $\text{Al}_6(\text{FeMn})$  phase, which had a share below the percentage (0.79%). The resulting values of the percentage evaluation of shares of individual phases are average values calculated from twenty measurements.

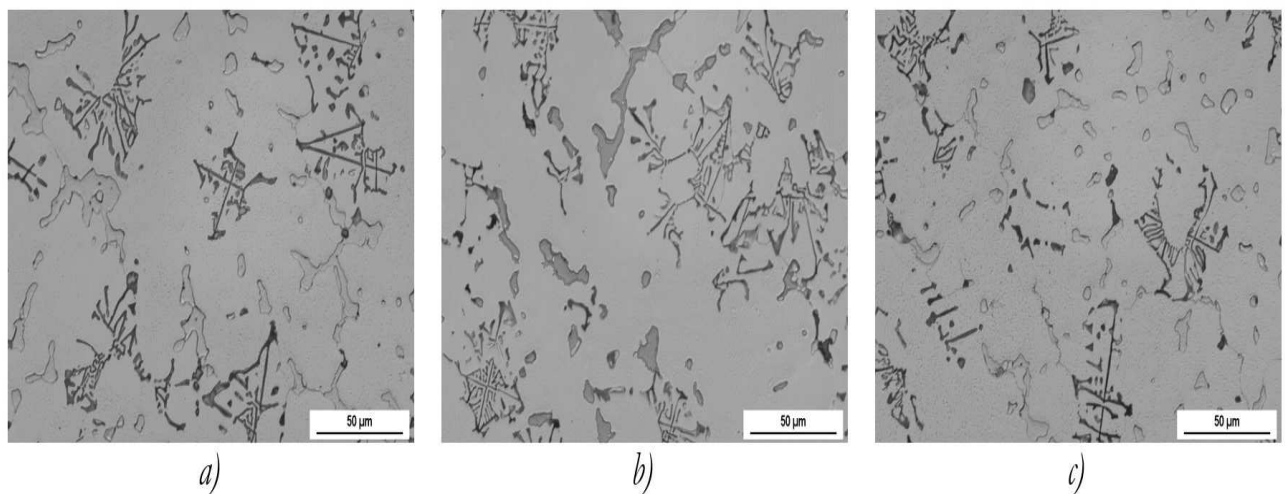


**Fig. 3** A percentage assessment of phases in the aluminum cast alloy, a) a share of  $\text{Mg}_2\text{Si}$ , b) a share of  $\text{Al}_3\text{Mg}_2$ , c) a share of  $\text{Al}_6(\text{FeMn})$

### 3 Fatigue tests

Fatigue tests (using the three-point bending test method) were performed on the ZWICK/ROELL AMSLER 150 HFP 5100 testing device (Fig. 4) according to norm STN 42 0363. This device uses the resonance principle with different amplitude (constant or variable) and mean load. Simple specimens (without notches) were loaded by three-point bending cyclic loading with conditions: static preload force

$F_{\text{static}} = -6 \text{ kN}$ , dynamic force  $F_{\text{dynamic}}$  varying from 4 kN up to 5.8 kN and the frequency of loading was approximately  $f = 100 \text{ Hz}$ . All tests were performed at a room temperature of  $22^\circ\text{C} \pm 5^\circ\text{C}$ . The value of  $2 \times 10^7$  numbers of cycles was set as reference and when specimen has reached this value without break, so called runout, that bending stress was considered as fatigue lifetime limit [12, 13].

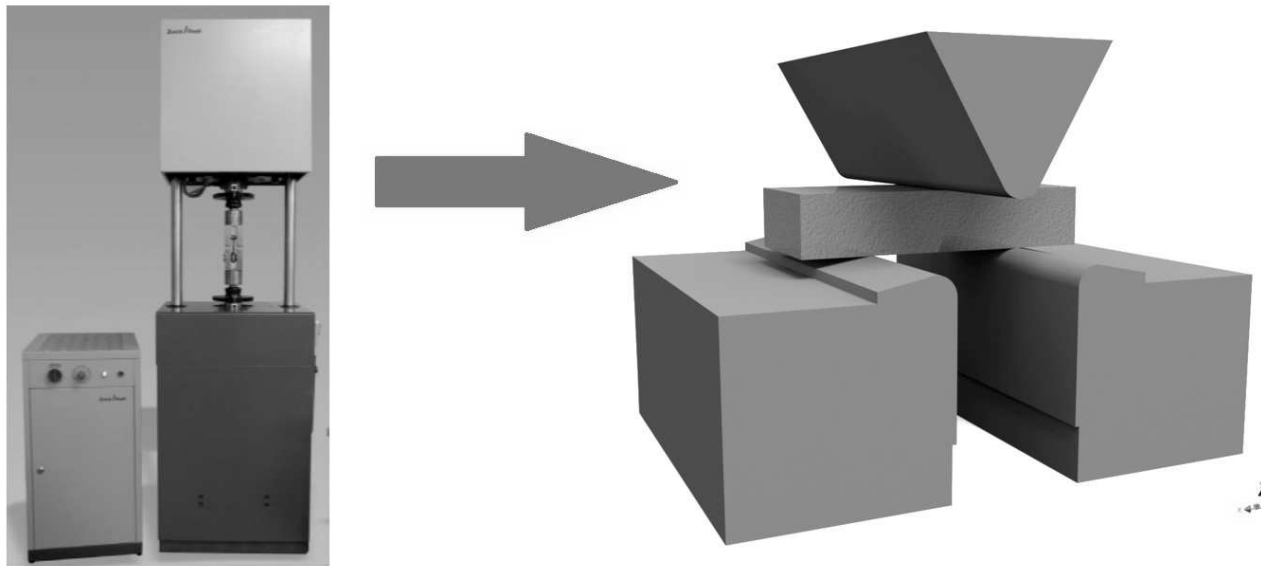


**Fig. 4** A fatigue experimental machine and a display of fatigue test method

## 4 Results and discussion

For the fatigue test, 20 specimens without notches were used. From results obtained from the fatigue tests, the curve (S-N curve) was constructed in semi-logarithmic coordinates (Fig. 5). From experimental results and especially from the constructed Wöhler curve, it can be seen that the fatigue life increases with

decreasing stress amplitude. Gray marks in the graph indicate specimens that have withstood a certain number of cycles under the selected load and the silver marks in the graph indicate specimens that did not fail before the maximum number of cycles, as runout. The result of fatigue test determined the limit number of cycles 20000010 at the maximum stress range  $\sigma_{\text{rmax}} = 273 \text{ MPa}$ .

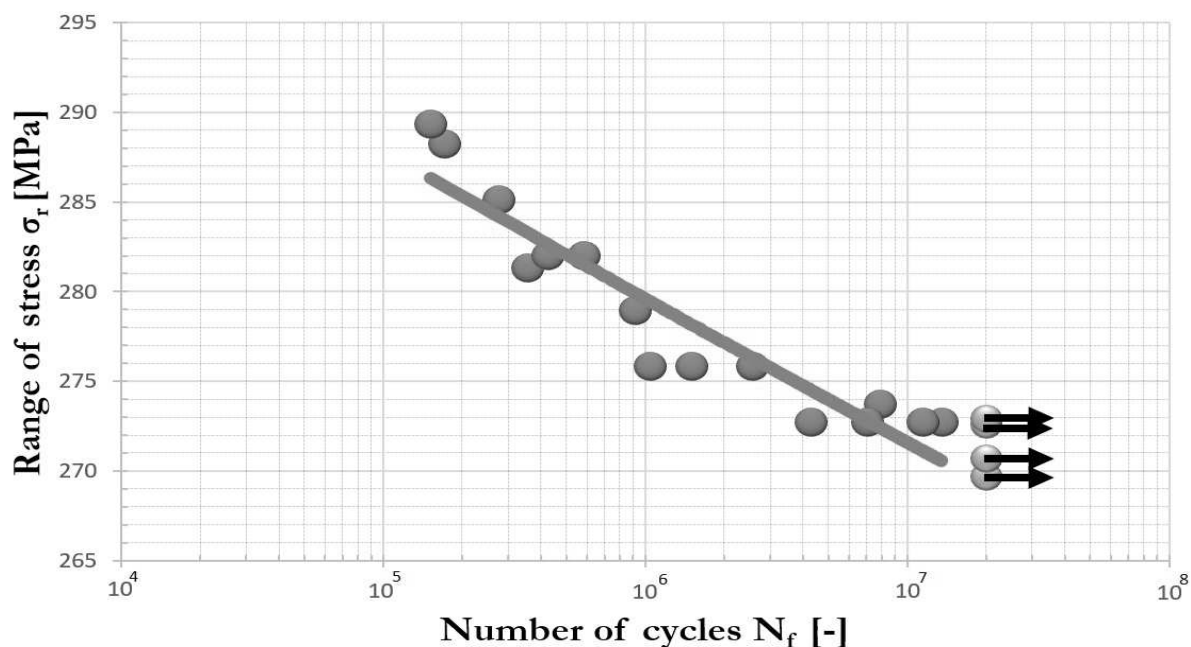


**Fig. 5** Results of fatigue tests for aluminum cast alloy AlMg9

## 5 Discussion

The microstructure of the aluminum cast alloy AlMg9 was expressively dendritic. The  $\alpha$ -phase (matrix of alloy) had the largest presence in the

structure. The publication from Boyko [14] reports that approximately  $2 \pm 0.4 \text{ wt.}\%$  of magnesium and  $0.38 \pm 0.05 \text{ wt.}\%$  of manganese are present in the solid matrix solution and the rest is made up of aluminum.

Since very little is described about this type of alloy (Al-Mg) (for example, much more is described about alloys of the type Al-Si, Al-Cu or Al-Zn), informations about phases found in the structure of the investigated alloy were mainly obtained from the publication from Vander Voort [15]. This publication states that phase such as  $\text{Al}_3\text{Mg}_2$ ,  $\text{Al}_6(\text{FeMn})$ ,  $\text{Mg}_2\text{Si}$  and  $\text{Al}_{18}\text{Mg}_3\text{Cr}_2$  can occur in Al-Mg cast alloys. Results of the experimental analyzes showed that  $\text{Mg}_2\text{Si}$ ,  $\text{Al}_3\text{Mg}_2$  and  $\text{Al}_6(\text{FeMn})$  phases were present in the alloy, which were mainly precipitated in interdendritic spaces. However, the presence of the  $\text{Al}_{18}\text{Mg}_3\text{Cr}_2$  phase in the structure was not confirmed by analysis, it was not there.

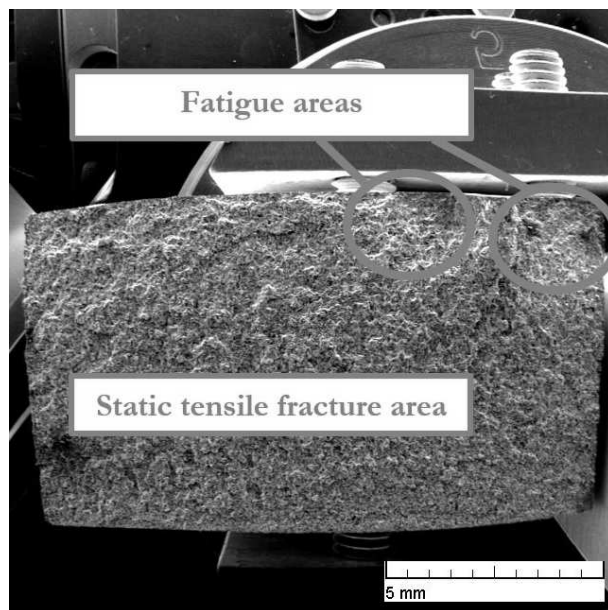


**Fig. 6** Fractography surface of aluminum cast alloy AlMg9 after fatigue test

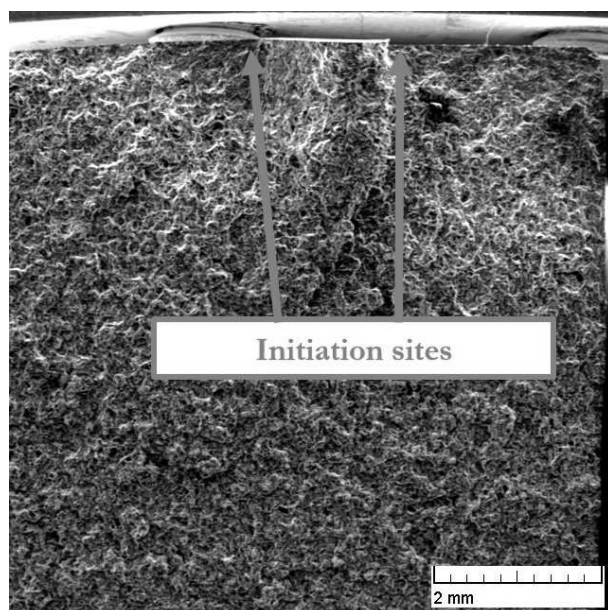


**Fig. 7** Fractography surface of aluminum cast alloy AlMg9 after fatigue test – two initiation points

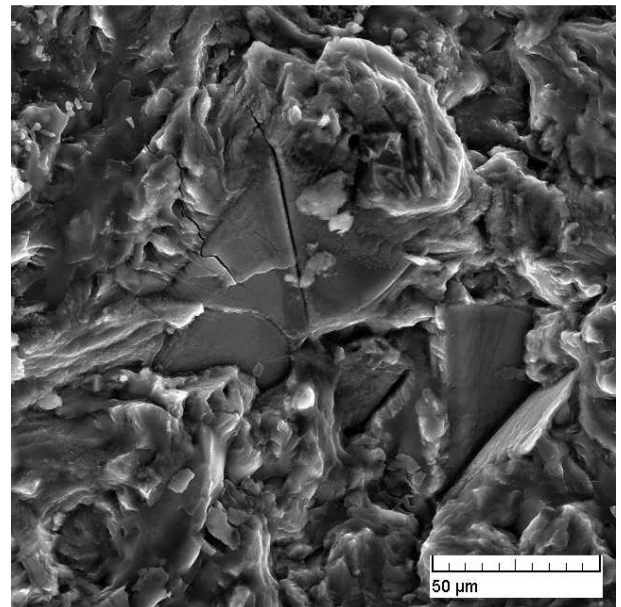


**Fig. 8** Transcrystalline fatigue failure of the  $\alpha$ -phase in the fatigue area

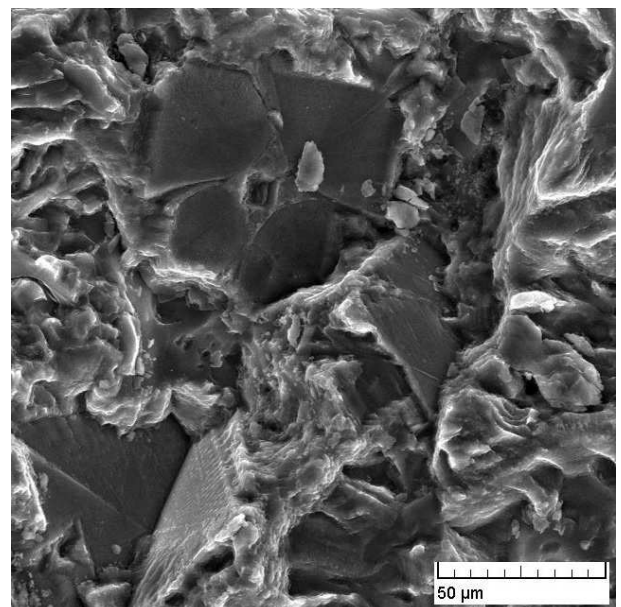


**Fig. 9** Transcrystalline fatigue failure of the  $\alpha$ -phase in the fatigue area (another place)

The experimental material was subjected to fractographic analysis after the fatigue tests. In this analysis, the fracture surfaces of specimens were observed using a TESCAN Vega II LMU scanning electron microscope [16, 17]. From the macrofractographic analysis of fracture surface of the specimen (Fig. 6), it is possible to determine the place of initiation or nucleation of the fatigue crack and also areas of individual fracture regions (namely the fatigue area and area of static fracture). A fatigue crack appeared on the surface of the specimen.

In the case of specimen which was observed, two initiation sites can be seen on the surface of the

fracture edge (Fig. 7). A larger number of initiation sites (more than one) occurs especially with higher load amplitudes. From this analysis, however, it was not possible to determine what was the cause of the fatigue crack.

From the microfractographic analysis, it can be seen that in the fatigue area (Fig. 8 and Fig. 9) it is characterized by many transcrystalline fatigue failures of the  $\alpha$ -phase. Intermetallic phases were an interphase failure in this area, at the matrix-phase interface. Typical fatigue features in this area, striations, could be observed in the specimen (Fig. 10).

A transcrystalline ductile fracture with dimple morphology and with plastically deformed ridges is typical for  $\alpha$ -phase rupture in the area of a static fracture (Fig. 11). Intermetallic phases were also an interphase failure in this region.

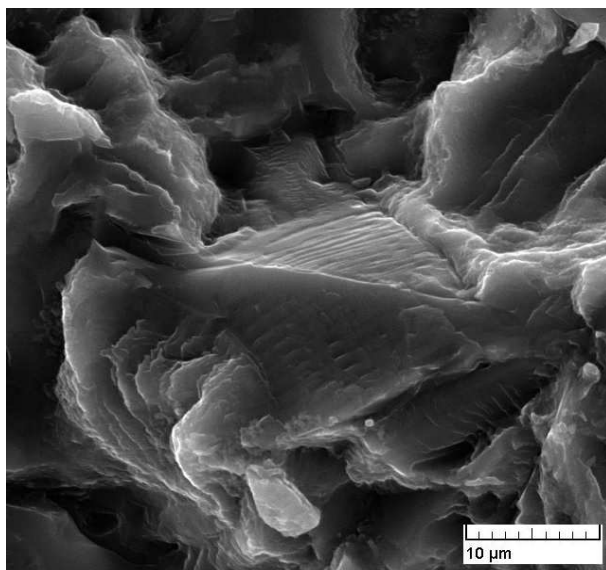


**Fig. 10** Typical fatigue features (striations) in the fatigue area

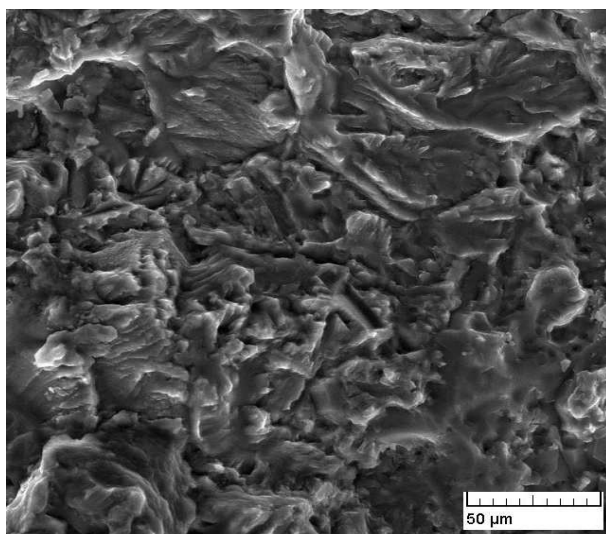


**Fig. 11** Fractography surface of aluminum cast alloy AlMg9 after fatigue test – static part of fatigue fracture

## 6 Conclusions

This manuscript provides information about aluminum alloy AlMg9, more specifically about the internal structure of material and fractographic analysis of fracture surface. The structure was evaluated in the initial state and the fractographic evaluation was performed after fatigue tests by three-point cyclic bending. A Wöhler curve (S-N curve) was constructed from the experimentally measured values. It is clear from it that the fatigue life decreases with increasing stress amplitude. The Wöhler curve appears to decrease steadily with increasing lifetime (with increasing number of cycles). The limit number of cycles  $2.10^7$  (20000010) was achieved at maximum stress range  $\sigma_{\text{rmax}} = 273$  MPa.

From fractographic analysis of fracture surfaces of specimens, it was not possible to determine from what the fatigue crack initiated, what was the exact cause. It is assumed that this could have been caused by either machining (milling) notches or by intermetallic phases acting in the alloy as stress concentrators where a fatigue crack could form. Microstructural analysis did not show the presence of pores that arise from casting defects, therefore pores were definitely not the cause of crack initiation.

## Acknowledgement

*The research was supported by the Scientific Grant Agency of the Ministry of Education of Slovak Republic and Slovak Academy of Sciences, VEGA 01/0134/20, VEGA 01/0398/19, KEGA 016ŽU-4/2020, and projects to support young researchers at UNIZA, the ID of projects 14877 and 12715. This article was also funded by the University of Žilina project 313011ASY4 – “Strategic implementation of additive technologies to strengthen the intervention capacities of emergencies caused by the COVID-19 pandemic.”*

## References

- [1] SNOPIŃSKI, P., KRÓL, M., TAŃSKI, T., KRUPIŃSKA, B. (2018). Effect of cooling rate on microstructural development in alloy AlMg9. In: *Journal of Thermal Analysis and Calorimetry*, Vol. 133, pp. 379-390. ISSN 1388-6150
- [2] SNOPIŃSKI, P., TAŃSKI, T., KRZYSZTOF, L., RUSZ, S., JONSTA, P., KRÓL, M. (2016). Wrought aluminium-magnesium alloys subjected to SPD processing. In: *International Journal of Materials Research*, Vol. 107, pp. 637-645. ISSN 2195-8556
- [3] BRITO, C., REINHART, G., NGUYEN-THI, H., MANGELINCK-NOEL, N., CHEUNG,

- N., SPINELLI, J.E., GARCIA, A. (2015). High cooling rate cells, dendrites, microstructural spacing and microhardness in a directionally solidified Al-Mg-Si alloy. In: *Journal of Alloys and Compounds*, Vol. 636, pp. 145-149. ISSN 0925-8388
- [4] BRODARAC, Z.Z., UNKIĆ, F., MEDVED, J., MRVAR, P. (2012). Determination of solidification sequence of the AlMg9 alloy. In: *Kovove Materialy*, Vol. 50, No. 01, pp. 59-67. Slovak Republic. ISSN 1338-4252
- [5] VIDAL, C., BAPTISTA, R., INFANTE, V. (2018). Numerical simulations of the fatigue behaviour of a friction stirred channel aluminium alloy. In: *MATEC Web of Conference*, 165, 21008. eISSN 2261-236X
- [6] CHENG, W., CHENG, H.S., MURA, T., KEER, L.M. (1994). Micromechanics modeling of crack initiation under contact fatigue. In: *Journal of Tribology*, Vol. 116, No. 1, pp. 2-8. ISSN 0742-4787
- [7] ZYCH, J., PIEKLO, J., MAJ, M., GARBACZ-KLEMPKA, A., PIEKOŚ, M. (2019). Influence of structural discontinuities on fatigue life of 4XXX0-series aluminum alloys. In: *Archives of Metallurgy and Materials*, Vol. 64, No. 2, pp. 765-771. ISSN 1733-3490
- [8] UHRÍČIK, M., PALČEK, P., CHALUPOVÁ, M., FRKÁŇ, M. (2018). The influence of the structure on the fatigue properties of aluminium alloys for the casting. In: *MATEC Web of Conference*, 157, 07013. eISSN 2261-236X
- [9] MIKOLAJČÍK, M., TILLOVÁ, E., KUCHARIKOVÁ, L., PASTIEROVIČOVÁ, L., CHALUPOVÁ, M., UHRÍČIK, M., ŠURDOVÁ, Z. (2022). Effect of higher iron content and manganese addition on the corrosion resistance of AlSi7Mg0.6 secondary alloy. In: *Manufacturing Technology*, Vol. 22, No. 4, pp. 436-443. UJEP. Czech Republic. ISSN 1213-2489.
- [10] BELAN, J., UHRÍČIK, M., HANUSOVÁ, P., VAŠKO, A. (2020). The Ti6Al4V alloy microstructure modification via various cooling rates, its influence on hardness and microhardness. In: *Manufacturing Technology*, Vol. 20, No. 5, pp. 560-565. UJEP. Czech Republic. ISSN 1213-2489.
- [11] ŠURDOVÁ, Z., KUCHARIKOVÁ, L., TILLOVÁ, E., PASTIEROVIČOVÁ, L., CHALUPOVÁ, M., UHRÍČIK, M., MIKOLAJČÍK, M. (2022). The influence of Fe content on corrosion resistance of secondary AlSi7Mg0.3 cast alloy with increased Fe-content. In: *Manufacturing Technology*, Vol. 22, No. 5, pp. 598-604. UJEP. Czech Republic. ISSN 1213-2489.
- [12] BELAN, J., VAŠKO, A., KUCHARIKOVÁ, L., TILLOVÁ, E. (2018). The fractography analysis of IN718 alloy after three-point flexure fatigue test. In: *MATEC Web of Conference*, 157, 07001. eISSN 2261-236X.
- [13] BELAN, J., KUCHARIKOVÁ, L., TILLOVÁ, E., CHALUPOVÁ, M. (2019). Three-point bending fatigue test of TiAl6V4 titanium alloy at room temperature. In: *Advances in Materials Science and Engineering*, 2019, 2842416. ISSN 1687-8434
- [14] BOYKO, V., LINK, T., MYKHALENKOV, K. (2014). Structure characterization and precipitation in two Al-Mg-Si-Mn casting alloys. In: *Metallurgy and Foundry Engineering*, Vol. 40, No. 3, pp. 111-124. ISSN 1230-2325.
- [15] VANDER VOORT, G.F. (2004). ASM Handbook Volume 9: Metallography and Microstructures. ASM International, USA. ISBN 0-87170-706-3.
- [16] TILLOVÁ, E., CHALUPOVÁ, M., ZÁVODSKÁ, D., KUCHARIKOVÁ, L., BELAN, J., VAŠKO, A. (2018). Effect of Al<sub>5</sub>FeSi phases in secondary AlZn10Si8Mg cast alloys on mechanical properties and fracture surface. In: *Manufacturing Technology*, Vol. 18, No. 6, pp. 1034-1040 UJEP. Czech Republic. ISSN 1213-2489.
- [17] ZÁVODSKÁ, D., TILLOVÁ, E., KUCHARIKOVÁ, L., CHALUPOVÁ, M. (2016). Fractography evaluation of fracture surfaces of aluminium alloy after fatigue tests. In: *Manufacturing Technology*, Vol. 16, No. 5, pp. 1199-1204. UJEP. Czech Republic. ISSN 1213-2489.